Back to Einstein: how to include burial in fluvial sediment diffusion models?

James K. Pierce [1]**and Marwan A. Hassan**[1]

[1]Department of Geography
University of British Columbia

Key Points:

- We develop a random-walk model of objects in intermittent transport through an environment with traps
- Its solution provides three ranges of diffusion, two of which are anomalous
- We apply the model to sediment transport in rivers to clarify the scale-dependence of bedload diffusion

Corresponding author: James Kevin Pierce, kpierce@alumni.ubc.ca

Abstract

Sediment grains transport through gravel-bed rivers in cycles of motion and rest. When grains rest on the surface, material transported from upstream can bury them. Grains on the surface shield buried grains from the flow, so they can be immobile for long time periods. These immobile periods can dominate sediment diffusion characteristics. Despite the significant impact of sediment burial on diffusion, nearly all existing models neglect it. In this letter, we present a random walk model incorporating sediment burial and solve it analytically. The model predicts three sediment diffusion ranges with distinct scaling characteristics in each. We relate the crossover times dividing these ranges to measurable transport parameters and describe each range from underlying physical processes. Our developments provide new geophysical perspective on the scale-dependence of fluvial sediment transport.

1 Introduction

Anomalous diffusion has attracted considerable research attention in recent times, emerging in diverse contexts including the transport of cholesterols through lipid bilayers (Jeon, Monne, Javanainen, & Metzler, 2012; Molina-Garcia et al., 2018), contaminants through soils (Berkowitz, Cortis, Dentz, & Scher, 2006; X. R. Yang & Wang, 2019), and pollinator insects through ecosystems (Reynolds & Rhodes, 2009; Vallaeys, Tyson, Lane, Deleersnijder, & Hanert, 2017). In this letter, we study anomalous diffusion in a river science context, where it emerges from the transport of coarse bedload sediment through river channels (Bradley, 2017; Martin, Jerolmack, & Schumer, 2012). H. A. Einstein (1937) developed the first model of bedload diffusion to describe his comprehensive experiments tracing painted grains through a flume in Meyer-Peter's laboratory (Ettema & Mutel, 2004). Diffusion is the spreading apart of grains as they transport downstream, and it is induced by differences in the transport characteristics of one grain and the next. Diffusion is usually quantified by the time dependence of the positional variance $\sigma_x^2(t)$ of a population. When $\sigma_x^2 \propto t$, the diffusion is said to be normal, since this is found in the classic diffusion problems (e.g. A. Einstein, 1905; Taylor, 1920). However, many transport phenomena show $\sigma_x^2 \propto t^\gamma$ with $\gamma \neq 1$. This diffusion is said to be anomalous (Sokolov, 2012). If $\gamma > 1$, it is said to be super-diffusive; while if $\gamma < 1$, it is said to be sub-diffusive (Metzler & Klafter, 2000). Einstein concluded from his experiments and modeling that bedload transport expresses normal diffusion.

Researchers after Einstein have come to recognize that coarse sediment moving through river channels can show either anomalous or normal diffusion depending on the timescale of observation (Nikora, Habersack, Huber, & McEwan, 2002). This is a significant issue since it implies diffusion models should be scale dependent, and it renders experimental data contingent on their observation timescales. Nikora et al. (2002); Nikora, Heald, Goring, and McEwan (2001) were the first to fundamentally rework Einstein's concept of bedload diffusion. They identified three ranges of diffusion from Newtonian simulations and experimental data, and they termed these ranges local, intermediate, and global in order of increasing timescale. They determined that σ_x^2 scales with a different power of time in each range, and they concluded this scaling could be either anomalous or normal. More recent works have more or less supported the Nikora et al. findings. Various numerical approaches show two (e.g. Fan, Singh, Guala, Foufoula-Georgiou, & Wu, 2016) or three (e.g. Bialik, Nikora, & Rowiński, 2012; Zhang, Meerschaert, & Packman, 2012) ranges of diffusion; one set of flume experiments appears to show two ranges of sediment diffusion (Martin et al., 2012), and several field studies have shown anomalous diffusion (Bradley, 2017; Phillips, Martin, & Jerolmack, 2013) However, the full picture of scale-dependent bedload diffusion is far from clear. In particular, we are not able to (super/normal/subdiffusion) of each range (local/intermediate/global), and no model has been developed, to our knowledge,

that derives all three diffusion ranges from process-based concepts of fluvial sediment transport.

In this letter, we develop a model of bedload diffusion which describes the local, intermediate, and global ranges of diffusion introduced by Nikora et al. by generalizing the original diffusion model of H. A. Einstein (1937). Einstein's model has been highly influential in river geophysics and has fostered an entire paradigm of research that leverages and generalizes his stochastic methods (e.g. Gordon, Carmichael, & Isackson, 1972; Hubbell & Sayre, 1964; Nakagawa & Tsujimoto, 1976; C. T. Yang & Sayre, 1971; Yano, 1969). His model's essential content is that individual grains move in instantaneous steps interrupted by durations of rest which lie on statistical distributions (Hassan, Church, & Schick, 1991). Einstein's model can be viewed as a special case of the continuous time random walk (CTRW) developed by Montroll and Weiss (1965) in condensed matter physics to describe the diffusion of charge carriers in solids. Our generalization of Einstein's model has two components. First, we include the duration and velocity of motions in place of instantaneous steps, and second, we add in the process of sediment burial, which has been associated with anomalous diffusion at long timescales (e.g. Bradley, 2017; Martin, Purohit, & Jerolmack, 2014). To develop this generalization, we leverage the multi-state CTRW developed by Weiss (1976, 1994) that extends the CTRW of Montroll and Weiss (1965). Below, we present the model in section 2 and solve it in section 3. Finally, we discuss the predictions of our model and its implications for scale-dependent bedload transport in sections 4 and 5.

2 Bedload diffusion with burial as a multi-state random walk

Consider a three-state random walk where the states are motion, rest, and burial. Label these as $i = 2$ (motion), $i = 1$ (rest), and $i = 0$ (burial). Our development of the governing equations for the three-state walk closely follows Weiss (1994), and our incorporation of the sediment burial process is similar to Schmidt, Sagués, and Sokolov (2007). In our model, times spent moving or resting on the bed surface are random variables characterized by exponential distributions, and movements have a constant velocity v. We consider burial to be a permanent condition which has some probability to occur when grains resting on the surface are covered by transported sediment. The probability of burial per unit time (burial rate) is considered constant, so the probability that a grain becomes buried increases with the time it rests.

A central concept in our derivation is the idea of a sojourn in the state i (Weiss, 1994). When a grain enters a state i at some time t_0 and position x_0, then leaves a state at some other time t_1 and position x_1, we say that the grain has completed a sojourn in the state i. The joint probability density for a complete sojourn in the state i of time $t = t_1 - t_0$ and displacement $x = x_1 - x_0$ is denoted $g_i(x, t)$. Similarly, we can consider incomplete sojourns. If a grain begins a sojourn in the state i at (t_0, x_0) and the sojourn is still on-going, the joint probability density to find the grain at (x_1, t_1) is $G_i(x, t)$. The g_i and G_i can be further decomposed when time and space components of the motion are independent (Weiss, 1994). We refer to g_i and G_i as the complete and incomplete propagators, since they move probability through space-time and are associated respectively with complete and incomplete sojourns.

Our target is the probability distribution $p(x, t)$ to find a grain at x, t if we know it started at $(x, t) = (0, 0)$; that is, if it started with the initial distribution $p(x, 0) = \delta(x)$. We denote the initial probabilities to be at rest or in motion as θ_1 and θ_2. Normalization requires $\theta_1 + \theta_2 = 1$. Our derivation has two main steps. First, we introduce and solve for a set of joint probabilities associated with transitions of a grain from one state to another. Second, we use these quantities to solve for the probabilities that a grain is in state i having position x at time t. Afterward, we sum

the latter probabilities over all states i to derive the joint probability that a grain is in any state at (x,t).

Now we begin the first stage of the derivation. Grains at rest may be trapped by burial. For simplicity, we consider burial to be permanent (e.g. Wu et al., 2019), and we assume grains resting on the surface can be buried with constant probability per unit time κ. Equivalently, we could say the mean time required for a resting grain to become buried is $1/\kappa$. From this assumption, the probability that a grain is not trapped after a time t at rest obeys a survival function $\Phi_F(t) = e^{-\kappa t}$ (F is for "free"). Likewise, the probability that it is trapped after resting for a time t is the complement $\Phi_T(t) = 1-\Phi_F(t)$ (T is for "trapped"). We introduce $\omega_{1T}(x,t)$, $\omega_{1F}(x,t)$, and $\omega_2(x,t)$ as the joint probabilities to find a grain at (x,t) having just completed a sojourn. The subscript $1T$ denotes the completion of a rest sojourn due to trapping by burial, while $1F$ denotes the completion of a rest sojourn due to motion. Similarly, the subscript 2 denotes the completion of a motion sojourn due to resting. Using an argument similar to Weiss (1994), we write integral equations to link the ω's:

$$\omega_{1T}(x,t) = \theta_1 \Phi_T(t) g_1(x,t) + \int_0^x dx' \int_0^t dt' \omega_2(x',t') \Phi_T(t-t') g_1(x-x', t-t'), \quad (1)$$

$$\omega_{1F}(x,t) = \theta_1 \Phi_F(t) g_1(x,t) + \int_0^x dx' \int_0^t dt' \omega_2(x',t') \Phi_F(t-t') g_1(x-x', t-t'), \quad (2)$$

$$\omega_2(x,t) \quad = \theta_2 g_2(x,t) + \int_0^x dx' \int_0^t dt' \omega_{1F}(x',t') g_2(x-x', t-t'). \quad (3)$$

The first equation can be understood as follows: $\omega_{1T}(x,t)$ describes the probability that a sojourn in the state 1 ends due to trapping at (x,t). This quantity has two contributions. The first contribution represents the possibility that the grain started at $(x,t) = (0,0)$ in the $i = 1$ state (with probability θ_1), propagated a distance x and a time t in the $i = 1$ state (with probability density $g_1(x,t)$), was trapped (with probability $\Phi_T(t)$), and is now at (x,t). The second contribution describes the possibility that the grain was in a motion sojourn which ended at (x',t') when it came to rest. From here, it propagated from (x',t') to (x,t) at rest (with probability density $g_1(x-x', t-t')$) and was trapped during this sojourn (with probability $\Phi_T(t-t')$). The reasoning is analogous for the other equations. The first terms denote the possibility that the grain was always in the sojourn from $t = 0$ while the second terms denote the possbility that the grain ended a sojourn in another state at (x',t'). Once the propagators are specified, we can solve (1-3) for the ω's. This completes the first stage of the derivation.

The second stage of our derivation involves the joint probabilities of being in state regardless of whether a sojourn has just completed. These are denoted by $p_0(x,t)$ (trapped), $p_1(x,t)$ (rest), and $p_2(x,t)$ (motion), and they involve the ω's for their definition:

$$p_0(x,t) = \int_0^t dt' \omega_{1T}(x, t-t'), \quad (4)$$

$$p_1(x,t) = \theta_1 G_1(x,t) + \int_0^x dx' \int_0^t dt' \omega_2(x',t') G_1(x-x', t-t'), \quad (5)$$

$$p_2(x,t) = \theta_2 G_2(x,t) + \int_0^x dx' \int_0^t dt' \omega_{1F}(x',t') G_2(x-x', t-t'). \quad (6)$$

Equation (4) says that grains buried at any (x,t) arrived there due to trapping at x at any time leading up to t. The reasoning in (5-6) is the same as for (1-3) except we use the propagators for incomplete sojourns. These equations can be solved once the propagators are specified and the ω's are known from (1-3). Finally, we form the total probability density for a grain to be found at (x,t) in any state. This is simply

$$p(x,t) = p_0(x,t) + p_1(x,t) + p_2(x,t). \quad (7)$$

This joint density is completely determined once (1-6) are solved.

3 Specification of propagators and solution of model

We consider sojourns in the rest state to occur for an exponentially distributed time interval given by the distribution $\psi_1(t) = k_1 e^{-k_1 t}$. The probability that a sojourn in this state lasts for at least a time t is then $\Psi_1(t) = \int_t^\infty \psi_1(t)dt = e^{-k_1 t}$. $1/k_1$ is the mean duration of a single rest. Since grains do not move in the rest sojourn, the probability density that a grain is displaced by a distance x in the rest sojourn in $\delta(x)$. Hence the complete propagator for rest sojourns is $g_1(x,t) = \delta(x)\psi_1(t)$, or

$$g_1(x,t) = \delta(x)k_1 e^{-k_1 t}. \tag{8}$$

Likewise, the incomplete propagator for a rest sojourn is $G_1(x,t) = \delta(x)\Psi_1(t) = \delta(x)e^{-k_1 t} = g_1(x,t)/k_1$. The motion propagators are reasoned similarly. We consider motions to occur with a constant velocity v and to have an exponentially distributed duration given by $\psi_2(t) = k_2 e^{-k_2 t}$. $1/k_2$ is the mean duration of a single motion. Since the velocity of motions is deterministic, the probability to find a grain at position x in a motion sojourn is $\delta(x - vt)$, and the complete propagator for motion sojourns is

$$g_2(x,t) = \delta(x - vt)k_2 e^{-k_2 t}, \tag{9}$$

while the incomplete propagator is $G_2(x,t) = g_2(x,t)/k_2$ as before.

Having defined the propagators, we set out to solve (1-6) and understand the bed-load diffusion expressed by the trapping model. The convolution structure of equations (1-6) presents a formidable problem. Luckily, we have the device of Laplace transforms. These project integro-differential equations into an alternate space in which convolutions are unraveled (e.g. Arfken, 1985). The double Laplace transform of a joint probability distribution $p(x,t)$ is defined by

$$\tilde{p}(\eta, s) = \int_0^\infty dx e^{-\eta x} \int_0^\infty dt e^{-st} p(x,t). \tag{10}$$

The Laplace-transformed moments of x are linked to derivatives of the double-transformed distribution (10) (cf. Berezhkovskii & Weiss, 2002). From equation (10) it's clear that

$$\langle \tilde{x}(s)^k \rangle = (-)^k \partial_\eta^k \tilde{p}(\eta, s)\Big|_{\eta=0}. \tag{11}$$

The operator $\langle \circ \rangle$ denotes the ensemble average (e.g. Kittel, 1958). This means we can compute the variance of position as $\sigma_x^2(t) = \langle x^2 \rangle - \langle x \rangle^2 = \mathcal{L}^{-1}\{\langle \tilde{x}^2 \rangle; t\} - \mathcal{L}^{-1}\{\langle \tilde{x} \rangle; t\}^2$, where $\mathcal{L}^{-1}$ denotes the inverse Laplace transform (e.g. Arfken, 1985). This is a powerful tool, since we can use it to derive the positional variance without integrating the distribution in equation (7).

Using the propagators (8-9) and this transform calculus, the joint distribution $p(x,t)$ is derived in appendix A, while the moments $\langle x \rangle$ and $\langle x^2 \rangle$ and ultimately the variance of position $\sigma_x^2(t)$ are derived in appendix B. With the shorthand notations $\xi = k_2 x/v$, $\tau = k_1(t - x/v)$, and $\Omega = (\kappa + k_1)/k_1$ (cf. Lisle et al., 1998), the joint distribution to find a grain at position x at time t is

$$\begin{aligned} p(x,t) = {} & \theta_1 \mathcal{H}(\xi)\mathcal{H}(\tau)\Big[1 - \frac{k_1}{\kappa + k_1}\Big(1 - e^{-(\kappa+k_1)t}\Big)\Big]\delta(x) \\ & + \frac{1}{v} e^{-\Omega\tau - \xi}\mathcal{H}(\xi)\mathcal{H}(\tau)\Big(\theta_1\Big[k_1 \mathcal{I}_0\big(2\sqrt{\xi\tau}\big) + k_2\sqrt{\frac{\tau}{\xi}}\mathcal{I}_1\big(2\sqrt{\xi\tau}\big)\Big] \\ & \quad + \theta_2\Big[k_1\delta(\tau) + k_2\mathcal{I}_0\big(2\sqrt{\xi\tau}\big) + k_1\sqrt{\frac{\xi}{\tau}}\mathcal{I}_1\big(2\sqrt{\xi\tau}\big)\Big]\Big) \\ & + \frac{1}{v}\frac{\kappa k_2}{\kappa + k_1} e^{-\kappa\xi/(\kappa+k_1)}\mathcal{H}(\xi)\mathcal{H}(\tau)\Big[(\theta_1/\Omega)\mathcal{P}_2(\xi/\Omega, \Omega\tau) + \theta_2\mathcal{P}_1(\xi/\Omega, \Omega\tau)\Big]. \end{aligned} \tag{12}$$

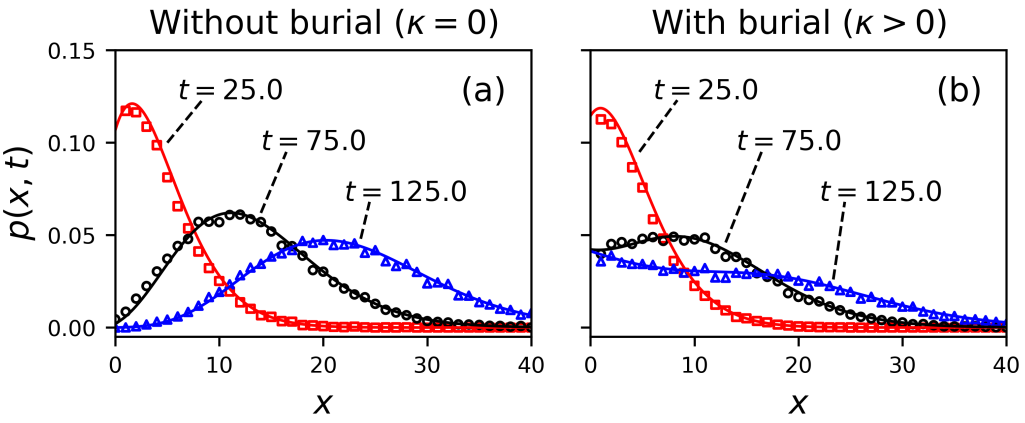

Figure 1. Joint distributions for a grain to be at position x at time t are displayed for the choice $k_1 = 0.1$, $k_2 = 1.0$, $v = 2.0$. Grains are considered initially at rest ($\theta_1 = 1$, $\theta_2 = 0$). The solid lines are the analytical distribution in equation (12), while the points are simulation results to show mathematical correctness. Colors pertain to different times. Units are unspecified, since our aim is to demonstrate the general characteristics of $p(x, t)$. Panel (a) shows the case $\kappa = 0$ – the absence of burial. In this case, the joint distribution tends toward Gaussian at large times (e.g. H. A. Einstein, 1937; Lisle et al., 1998). Panel (b) shows the case when grains have rate $\kappa = 0.01$ to become buried while resting. Because of burial, the joint distribution tends toward a more uniform distribution than Gaussian. This shows a redistribution of probability to smaller values of x due to the burial process (cf. Wu et al., 2019). The redistribution is encoded mathematically by the Marcum Q-function terms in equation (12). A similar tendency is seen in field studies of tracer dispersion in gravel bed rivers (e.g. Hassan & Church, 1994).

$\mathcal{H}$ is the Heaviside step function and we use the convention $\mathcal{H}(0) = 1$. The $\mathcal{I}_\nu$ are modified Bessel functions of the first kind, and the $\mathcal{P}_\mu$ are generalized Marcum Q-functions defined by $\mathcal{P}_\mu(x, y) = \int_0^y e^{-z-x}(z/x)^{(\mu-1)/2}\mathcal{I}_{\mu-1}(2\sqrt{xz})dz$ (Temme, 1996). Modified Bessel functions are common in one-dimensional diffusion problems (e.g. Daly & Porporato, 2010; H. A. Einstein, 1937; Giddings & Eyring, 1955).

The Marcum Q-functions are convolutions between modified Bessel functions and decaying exponentials. They were originally devised in relation to radar detection theory (Marcum, 1960). Conceptually, the Q-functions emerge in our context from the sediment burial process. According to our assumptions, resting grains can become buried in some interval of time with an exponential probability. Meanwhile, the probability that grains are resting follows a modified Bessel distribution (e.g. H. A. Einstein, 1937; Lisle et al., 1998). As a result, the probability that sediment is resting and becomes buried involves the convolution structure of the Marcum Q-functions. Consistent with this interpretation, the terms involving these convolutions vanish when the burial rate is taken to zero ($\kappa \to 0$). Figure 1 depicts the distribution (12) alongside simulations generated by a direct method based on evaluating the cumulative transition probabilities between states on a small timestep (cf. Barik, Ghosh, & Ray, 2006). A link to the simulation code, which includes descriptive comments, is available in the acknowledgments.

The first two moments and the positional variance are derived in appendix B. The moments are

$$\langle x(t)\rangle = A_1 e^{(b-a)t} + B_1 e^{-(a+b)t} + C_1, \tag{13}$$

$$\langle x^2(t)\rangle = A_2(t) e^{(b-a)t} + B_2(t) e^{-(a+b)t} + C_2. \tag{14}$$

In these equations, $a = (\kappa + k_1 + k_2)/2$ and $b = \sqrt{a^2 - \kappa k_2}$ are effective rates having dimensions of inverse time. The A_i, B_i, and C_i are polynomials available in table 1. The variance is

$$\sigma_x^2(t) = A(t) e^{(b-a)t} + B(t) e^{-(a+b)t} + C(t). \tag{15}$$

A, B, and C are transcendental functions available in table 1. This equation represents the scale-dependence of bedload diffusion for sediment gradually undergoing burial.

Table 1. Polynomials and transcendental functions used in the expressions of the mean (13), second moment (14) and variance (15) of bedload tracers.

$$A_1 = \frac{v}{2b}\Big[\theta_2 + \frac{k_1 + \theta_2\kappa}{b-a}\Big]$$

$$B_1 = -\frac{v}{2b}\Big[\theta_2 - \frac{k_1 + \theta_2\kappa}{a+b}\Big]$$

$$C_1 = -\frac{v}{2b}\Big[\frac{k_1 + \theta_2\kappa}{b-a} + \frac{k_1 + \theta_2\kappa}{a+b}\Big]$$

$$A_2(t) = \frac{v^2}{2b^3}\Big[(bt-1)[k_1 + \theta_2(2\kappa + k_1 + b - a)] + \theta_2 b + \frac{(\kappa + k_1)(\theta_2\kappa + k_1)}{(b-a)^2}[(bt-1)(b-a) - b]\Big]$$

$$B_2(t) = \frac{v^2}{2b^3}\Big[(bt+1)[k_1 + \theta_2(2\kappa + k_1 - a - b)] + \theta_2 b - \frac{(\kappa + k_1)(\theta_2\kappa + k_1)}{(a+b)^2}[(bt+1)(a+b) + b]\Big]$$

$$C_2 = \frac{v^2}{2b^3}(\kappa + k_1)(\theta_2\kappa + k_1)\Big[\frac{2b-a}{(b-a)^2} + \frac{a+2b}{(a+b)^2}\Big]$$

$$A(t) = A_2(t) - 2A_1C_1 - A_1^2 \exp[(b-a)t]$$

$$B(t) = B_2(t) - 2B_1C_1 - B_1^2 \exp[-(a+b)t]$$

$$C(t) = C_2 - C_1^2 - 2A_1B_1 \exp[-2at]$$

The positional variance is plotted in figure 2 for conditions $\theta_1 = 1$ and $k_2 \gg k_1 \gg \kappa$. We interpret "$\gg$" to mean "of at least an order of magnitude greater". These conditions mean that all grains are initially at rest (cf. Wu et al., 2019), motion intervals are typically much shorter than rests (cf. H. A. Einstein, 1937), and sediment burial requires a much longer time than typical rests. We concentrate on these conditions in this paper as they are most relevant to bedload diffusion in gravel-bed rivers, where sediment transport is typically rarefied and intermittent, and the burial process is relatively slow compared to surface resting times (e.g. Ferguson & Hoey, 2002; Hassan & Church, 1994). Figure 2 demonstrates that under these conditions the variance (15) shows three ranges of bedload diffusion with approximate power law scaling ($\sigma_x^2 \propto t^\gamma$), followed by a fourth range with no diffusion ($\sigma_x^2 = \text{const}$). We associate the first three ranges with the local, intermediate, and global ranges proposed by Nikora et al. (2002, 2001), and identify the fourth range as resulting from the burial of all sediment grains. We suggest to call the fourth range the geomorphic range, since any further transport in this range can occur only if scouring the bed exposes buried grains to

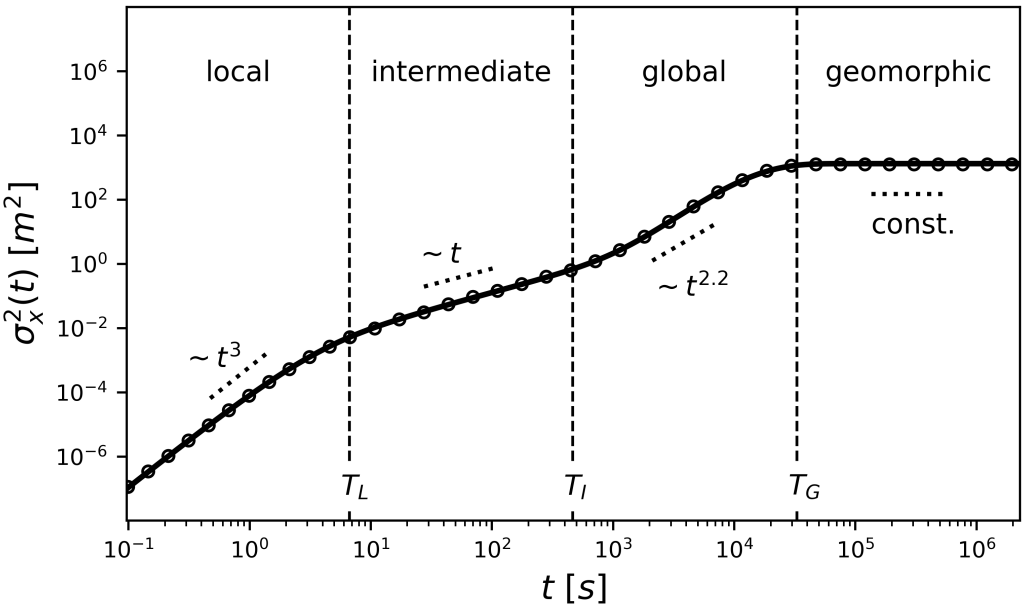

Figure 2. The variance equation (15) is plotted for the parameters $1/k_2 = 1.5$s, $1/k_1 = 30.0$s, and $v = 0.1$m/s. These values are comparable to laboratory flume experiments transporting small ($\sim$ 5mm) gravels (cf. Lajeunesse et al., 2010; Martin et al., 2012). The timescale of burial is set to $1/\kappa = 7200.0$s (two hours), and the initial condition is rest ($\theta_1 = 1$). The solid line is equation (15) while the points are directly simulated. When $k_2 \gg k_1 \gg \kappa$, as as is the case in this plot, there are four distinct scaling ranges of σ_x^2: local, intermediate, global, and geomorphic. Within each range, a slope key is added to demonstrate the scaling $\sigma_x^2 \propto t^\gamma$. There are three crossovers between these ranges, denoted on the figure by vertical lines. Crossover times T_L, T_I, and T_G are indicated at the bottom of the plot. They are given in equations (16-18) in terms of model parameters.

the flow (cf. Martin et al., 2014; Nakagawa & Tsujimoto, 1980; Voepel, Schumer, & Hassan, 2013). Using this terminology, we summarize when $k_2 \gg k_1 \gg \kappa$ and $\theta_1 = 1$, the variance in equation (15) expresses four scaling ranges of bedload diffusion: local, intermediate, global, and geomorphic. However, we should highlight the model's representation of the geomorphic range is unrealistic due to our simplifying assumption of permanent burial (cf. Wu et al., 2019). Properly modeling the geomorphic range requires investigations beyond the scope of this letter.

4 Discussion of scale-dependent bedload diffusion

The model we presented involves four parameters. These are the characteristic velocity v of moving sediment and three key timescales: $1/k_2$, $1/k_1$, and $1/\kappa$. The timescales represent the mean duration of motion, the mean duration of rest, and the mean duration of rest before burial occurs. As shown in figure 2, scaling laws $\sigma_x^2 \propto t^\gamma$ approximately characterize the diffusion in each scaling range. The exponents γ in each range result from competition between different terms in equation (15). Between these ranges, there are crossover regions where the scaling is not a simple power law. Because these crossover regions are relatively narrow, we can approximately characterize them with crossover times T_L, T_I, and T_G. These times partition the diffusion ranges into

$0 < t < T_L$ (local), $T_L < t < T_I$ (intermediate), $T_I < t < T_G$ (global), and $T_G < t$ (geomorphic). Figure 2 depicts these crossover times as vertical lines. To understand the scale dependence expressed by the bedload variance 15, we need to determine the exponents γ of each range and relate the crossover times T_L, T_I, and T_G between diffusion ranges to the model parameters v, k_1, k_2, and κ.

We determine the diffusion exponents γ in the local, intermediate, and global ranges using two limiting cases of equation (15): (1) $t \ll 1/\kappa$, and (2) $1/k_2 \to 0$ while $vk_2 = \text{const}$. Limit (1) corresponds to times so short a negligible amount of sediment burial has occurred, while limit (2) corresponds to times so long a motion interval appears as an instantaneous step having mean step length $l = vk_2$. We evaluate these limits in appendix C and obtain the diffusion exponents. Local range diffusion has exponent $2 \leq \gamma \leq 3$ depending on the initial conditions θ_1 and θ_2. When the initial conditions are pure, meaning one of the θ_i is zero, the local exponent is $\gamma = 3$. When grains start in a mixture of motion and rest states, meaning neither θ_i is zero, the local exponent is $\gamma = 2$. Intermediate range diffusion always has exponent $\gamma = 1$, agreeing with the classic flume experiments based on visually tracing painted stones (e.g. H. A. Einstein, 1937; Nakagawa & Tsujimoto, 1976; Yano, Tsuchiya, & Michiue, 1969). Finally, global range diffusion has exponent $1 \leq \gamma \leq 3$ depending on the ratio k_1/κ. In the extreme case $k_1/\kappa \approx 0$, we find normal diffusion $\sigma_x^2 \propto t$. However, in the opposite extreme $k_1/\kappa \to \infty$, we find super-diffusion $\sigma_x^2 \propto t^3$. For general values of the ratio κ/k_1, the global exponent lies between these extremes. For the parameters generating figure 2, the global range exponent is $\gamma \approx 2.2$. We surmise when the model parameters satisfy $k_2 \gg k_1 \gg \kappa$ meaning all three diffusion ranges exist, the variance (15) implies local range superdiffusion with exponent depending on the θ_i, intermediate range normal diffusion with no dependence on model parameters, and global range superdiffusion with exponent depending on the ratio k_1/κ. Finally, the model supports a geomorphic range of no diffusion ($\gamma = 0$) associated with the eventual and permanent trapping of all sediment grains.

Each crossover time relates to a physical process acting on a population of grains. Exchange between motion and rest states induces the local/intermediate crossover, the onset of sediment burial induces the intermediate/global crossover, and the completion of sediment burial induces the global/geomorphic crossover. Each process admits two characteristic times, and we formulate the crossover times heuristically as geometric averages of these characteristic times:

$$T_L = \sqrt{\frac{1}{k_1}\frac{1}{k_2}}, \tag{16}$$

$$T_I = \sqrt{\frac{1}{k_1}\frac{1}{\kappa}}, \tag{17}$$

$$T_G = \sqrt{\frac{1}{\kappa}\frac{k_1 + k_2}{\kappa k_1}}. \tag{18}$$

Figure 2 depicts these relationships as dashed vertical lines. The times $1/k_1$ and $1/k_2$ characterize exchanges between motion and rest, while $1/k_1$ and $1/\kappa$ characterize the onset of burial originating from grains buried within their first resting sojourns. Equations (16) and (17) mix these paired times. The completion of sediment burial originates from the last grains to bury. In one extreme, all grains rest on the surface, meaning the last grains bury around $1/\kappa$; while in another, some fraction of grains remains in motion for a long time and evades burial. By analogy to the mobile-immobile model of Ancey, Böhm, Jodeau, and Frey (2006), we reason a fraction $k_1/(k_1 + k_2)$ of the free population can be in motion and evading burial, and for this fraction we propose an effective trapping rate $\kappa k_1/(k_1+k_2)$. Equation (18) mixes the reciprocal of this effective rate with $1/\kappa$. We tested formulas (16-18) for many parameter choices and concluded they adequately represent the crossover locations between diffusion regimes provided the parameters satisfy $k_2 \gg k_1 \gg \kappa$ and grains start from rest ($\theta_1 = 1$).

However, starting grains from motion ($\theta_2 = 1$) widens the crossover region between local and intermediate ranges, meaning equation (16) loses representative power; while setting relatively very large values of k_2 widens the crossover region between global and geomorphic ranges, meaning equation (18) loses representative power. Ultimately, we emphasize the representation of finite width crossover regions by individual crossover times is an idealization, so we propose equations (16-18) as heuristics. These relations provide useful divisions between the bedload diffusion scaling ranges.

In this letter, we have developed a model extending earlier works to describe three ranges of bedload diffusion. The model reduces to earlier works through the two simplified limits previously leveraged to extract the scaling exponents γ. As discussed in appendix C, limit (1) implies the model developed by Lisle et al. (1998) to describe soil transport within a sheet flow, while limit (2) implies the model developed by Wu et al. (2019) to describe bedload transport with burial burial. Either of these limits further simplifies to the classic results of H. A. Einstein (1937) and his early followers (e.g. Hubbell & Sayre, 1964; Nakagawa & Tsujimoto, 1976; Yano, 1969) predicting a single range of normal diffusion. Lisle et al. (1998) generalized the Einstein model to include a finite velocity and duration of motion in place of instantaneous steps, and they derived two ranges of diffusion – super-diffusive and normal. Wu et al. (2019) developed an active layer formulation of bedload transport where grains are transferred from the active layer (surface) to the substrate layer (burial) at a constant rate. They simplified the problem by interpreting motions as instantaneous steps and derived two ranges of diffusion – normal and super-diffusive. Our model extends these two works and re-frames them in the formalism of multi-state CTRWs (e.g. Weiss, 1994) that was implicitly applied by H. A. Einstein (1937). Investigators aiming to push bedload diffusion models further might benefit from staying close to this physical formalism.

We offer several implications of our model for investigators of bedload diffusion in gravel-bed streams. First, our model confines the valid range of scale-independent models such as the advection-diffusion equation (e.g. Ganti, Meerschaert, Foufoula-Georgiou, Viparelli, & Parker, 2010) and the Einstein model (e.g. Martin et al., 2012) for practical applications such as contaminant transport (e.g Macklin et al., 2006; Malmon, Reneau, Dunne, Katzman, & Drakos, 2005) and aquatic habitat restoration (e.g. Gaeuman, Stewart, Schmandt, & Pryor, 2017) where bedload diffusion predictions are often required. When the observation timescale satisfies $T_L < t < T_I$, with T_L and T_I given by equations (16) and (17), we anticipate normal bedload diffusion $\sigma_x^2 = D_d t$. Second, the model links bedload transport understanding across scales. In practice, we might measure sediment diffusion within a channel on one timescale with intent to apply our knowledge at smaller or larger timescales; usually, experimental methods constrain the measurement timescale. For example, we could determine k_1 and k_2 by measuring the virtual velocity and diffusivity of sediment tracers in the intermediate range (e.g. H. A. Einstein, 1937; Nakagawa & Tsujimoto, 1976; Yano et al., 1969), although experimental limitations prevent any measurement of global range characteristics. With an estimate of the trapping rate κ, equation 15 provides diffusion characteristics of the global range $T_I < t < T_G$ which is more difficult to study experimentally.

Finally, we highlight some limitations of our model and suggest topics for further research. Two limitations of our model are its treatment of sediment burial as a permanent condition and its assumption that burial is the only trapping process affecting bedload transport. In actuality, burial is a temporary condition linked to scour and fill of the sedimentary bed (Ferguson, Bloomer, Hoey, & Werritty, 2002; Hassan & Church, 1994; Martin et al., 2014; Voepel et al., 2013), and other trapping processes have been identified in field experiments: for example, varying water depths strand sediment on bars and floodplains (e.g. Bradley, 2017; Ferguson et al., 2002; Malmon, Dunne, & Reneau, 2003). These two limitations point to deeper inadequacies in contemporary

river science understanding and suggest several topics in need of more study. First, many contemporary experiments on resting times have attributed resting times to any non-moving sediment whether trapped or not, and this is known to imply heavy-tailed sediment resting time distributions (e.g. Bradley, 2017; Martin et al., 2012; Olinde & Johnson, 2015). Up to now, there have been very few experimental studies which resting times while accounting for their mechanism (cf. Martin et al., 2014). would provide the required foundation to overcome one limitation of the present work and include additional trapping processes into bedload diffusion models. Second, the role of channel morphology and unsteady flows remains essentially untouched in stochastic models of bedload transport.

Finally, we note a limitation of our model which remains an entirely open problem in stochastic modelling. the role of channel morphology and its evolution on statistical characteristics of sediment transport are experimentally well-known and appreciable (e.g. Hassan & Bradley, 2017; Kasprak, Wheaton, Ashmore, Hensleigh, & Peirce, 2014; Pyrce & Ashmore, 2005) this imparts spatial and temporal variations into these statistics, or it possibly renders them ill-defined, which would be an unfortunate state of affairs.

Finally, with regard to these limitations we highlight that the random walk formalism from the physics literature we have used in this letter (Weiss, 1994) has been carefully extended to conditions where mobility characteristics vary across space and time. This is called a random walk in a random environment and is a popular concept in biological transport (e.g. Codling, Plank, & Benhamou, 2008). Perhaps there are lessons in this literature for river geophysics. Can the morphologically active river channel be treated as a random environment while bedload grains move in random walks?

5 Conclusion

We have developed a random walk model between alternating mobile and immobile states with a possibility of trapping from the immobile state, and we have used it to describe the diffusion of bedload sediment transporting through a river channel as it gradually becomes buried. This ultimately extends the original diffusion model of H. A. Einstein (1937). To our knowledge, this model is the first analytical description of bedload diffusion across local, intermediate, and global timescales. Pushing the ideas of Nikora et al. (2002) somewhat further, we have suggested a geomorphic range of diffusion to describe the range at timescales larger than the global range that is not properly characterized by existing models of bedload diffusion that neglect morphodynamic processes. Our model implies a possibility to use information from experiments conducted on one timescale to understand sediment diffusion phenomena and related problems such as channel morphology (e.g. Church, 2006; Hassan & Bradley, 2017) and environmental issues (e.g. Gaeuman et al., 2017; Macklin et al., 2006) on other timescales. The next step to incorporate the bed scour process which re-exposes buried sediment into a bedload diffusion model like the one we have presented here. This will overcome the approximation of permanent burial and better resolve the diffusion characteristics of the geomorphic range. The multi-state random walk formalism we used here should readily accommodate this extension (e.g. Weiss, 1994) and others aiming to incorporating more physical processes into Einstein's modeling paradigm of fluvial sediment diffusion.

A Calculation of the distribution function

Double transforming (1-3) using the definition (10) gives

$$\tilde{\omega}_{1T}(\eta,s) = \theta_1\tilde{g}_1(\eta,s) + \tilde{\omega}_2(\eta,s)\tilde{g}_1(\eta,s) - \tilde{\omega}_{1F}(\eta,s), \tag{A.1}$$
$$\tilde{\omega}_{1F}(\eta,s) = \theta_1\tilde{g}_1(\eta,s+\kappa) + \tilde{\omega}_2(\eta,s)\tilde{g}_1(\eta,s+\kappa), \tag{A.2}$$
$$\tilde{\omega}_2(\eta,s) \;\; = \theta_2\tilde{g}_2(\eta,s) + \tilde{\omega}_{1F}(\eta,s)\tilde{g}_2(\eta,s). \tag{A.3}$$

This purely algebraic system solves for

$$\tilde{\omega}_{1T}(\eta,s) = \frac{\theta_1+\theta_2\tilde{g}_2(\eta,s)}{1-\tilde{g}_1(\eta,s+\kappa)\tilde{g}_2(\eta,s)}\big\{\tilde{g}_1(\eta,s)-\tilde{g}_1(\eta,s+\kappa)\big\}, \tag{A.4}$$
$$\tilde{\omega}_{1F}(\eta,s) = \frac{\theta_1+\theta_2\tilde{g}_2(\eta,s)}{1-\tilde{g}_1(\eta,s+\kappa)\tilde{g}_2(\eta,s)}\tilde{g}_1(\eta,s+\kappa), \tag{A.5}$$
$$\tilde{\omega}_2(\eta,s) \;\; = \frac{\theta_2+\theta_1\tilde{g}_1(\eta,s+\kappa)}{1-\tilde{g}_1(\eta,s+\kappa)\tilde{g}_2(\eta,s)}\tilde{g}_2(\eta,s). \tag{A.6}$$

Double transforming (4-6) gives

$$\tilde{p}_0(\eta,s) = \frac{1}{s}\tilde{\omega}_{1T}(\eta,s), \tag{A.7}$$
$$\tilde{p}_1(\eta,s) = \theta_1\tilde{G}_1(\eta,s) + \tilde{\omega}_2(\eta,s)\tilde{G}_1(\eta,s), \tag{A.8}$$
$$\tilde{p}_2(\eta,s) = \theta_2\tilde{G}_2(\eta,s) + \tilde{\omega}_{1F}(\eta,s)\tilde{G}_2(\eta,s). \tag{A.9}$$

The total probability is $p(x,t) = p_0(x,t)+p_1(x,t)+p_2(x,t)$. Using equations (A.4-A.9) this becomes, in the double Laplace representation,

$$\begin{aligned}\tilde{p}(\eta,s) = \frac{1}{s}&\frac{\theta_1+\theta_2\tilde{g}_2(\eta,s)}{1-\tilde{g}_1(\eta,s+\kappa)\tilde{g}_2(\eta,s)}\big\{\tilde{g}_1(\eta,s)-\tilde{g}_1(\eta,s+\kappa)\big\}\\ &+\frac{\theta_1\big[\tilde{G}_1(\eta,s)+\tilde{g}_1(\eta,s+\kappa)\tilde{G}_2(\eta,s)\big]+\theta_2\big[\tilde{G}_2(\eta,s)+\tilde{g}_2(\eta,s)\tilde{G}_1(\eta,s)\big]}{1-\tilde{g}_1(\eta,s+\kappa)\tilde{g}_2(\eta,s)}.\end{aligned} \tag{A.10}$$

Plugging the propagators outlined in equations (8-9) into equation (A.10) gives

$$\tilde{p}(\eta,s) = \frac{1}{s}\frac{(s+\kappa+k')s+\theta_1(s+\kappa)\eta v+\kappa k_2}{(s+\kappa+k_1)\eta v+(s+\kappa+k')s+\kappa k_2}. \tag{A.11}$$

In this equation, $k' = k_1+k_2$, and we have used the normalization requirement of the initial probabilities $\theta_1+\theta_2 = 1$. The double inverse transform of this equation provides the distribution $p(x,t)$. It is convenient to invert the transform over η first. Using the results 15.103 (transform of exponential), 15.123 (transform of derivative), and 15.141 (transform of Dirac delta function) from Arfken (1985) provides

$$\begin{aligned}\tilde{p}(x,s) = \theta_1\frac{s+\kappa}{s(s+\kappa+k_1)}\delta(x) + \frac{1}{v}\Big(&\frac{(s+\kappa+k')s+\kappa k_2}{s(s+\kappa+k_1)}\\ &-\frac{\theta_1(s+\kappa)[s(s+\kappa+k_1)+\kappa k_2]}{s(s+\kappa+k_1)^2}\Big)\exp\Big[-\frac{(s+\kappa+k')s+\kappa k_2}{s+\kappa+k_1}\frac{x}{v}\Big].\end{aligned} \tag{A.12}$$

Taking the remaining inverse transform over s, applying results 15.152 (substitution), 15.164 (translation), and 15.175 (transform of te^{kt}) from Arfken (1985), and defining the shorthand notations $\tau = k_1(t-x/v)$, $\xi = k_2x/v$, and $\Omega = (\kappa+k_1)/k_1$, gives the simpler form

$$\begin{aligned}p(x,t) = \theta_1\Big[1-\frac{k_1}{\kappa+k_1}\big(1-e^{-(\kappa+k_1)t}\big)\Big]\delta(x) + \frac{1}{v}\exp[\Omega\tau-\xi]\\ \times\mathcal{L}^{-1}\Big\{\Big(\theta_2+\frac{\theta_1k_1+\theta_2k_2}{s}+\frac{\theta_1k_1k_2}{s^2}+\frac{\theta_2\kappa k_2}{s(s-\kappa-k_1)}+\frac{\theta_1\kappa k_1k_2}{s^2(s-\kappa-k_1)}\Big)\\ \times\exp\big[\frac{k_1\xi}{s}\big];\tau/k_1\Big\}.\end{aligned} \tag{A.13}$$

Using entries 2.2.2.1, 2.2.2.8, and 1.1.1.13 from Prudnikov, Brychkov, and Marichev (1992) in conjunction with the definition of the Marcum Q-function $\mathcal{P}_\mu(x,t)$ (e.g. Temme, 1996), and inserting the Heaviside functions to account for the fact that grains can neither travel backwards nor at speeds exceeding v, we finally arrive at equation 12 for the joint distribution $p(x,t)$.

B Calculation of the moments

We leverage equation 11 to compute the first two moments of position x and ultimately its variance. The first two derivatives of the double Laplace transformed distribution (A.11) are

$$\partial_\eta \tilde{p}(\eta,s) = -v\frac{1}{s}\frac{[(s+\kappa+k')s+\kappa k_2][\theta_2(s+\kappa)+k_1]}{[\eta v(s+\kappa+k_1)+(s+\kappa+k')s+\kappa k_2]^2}, \tag{B.1}$$

$$\partial_\eta^2 \tilde{p}(\eta,s) = 2v^2\frac{1}{s}\frac{(s+\kappa+k_1)[(s+\kappa+k')s+\kappa k_2][\theta_2(s+\kappa)+k_1]}{[\eta v(s+\kappa+k_1)+(s+\kappa+k')s+\kappa k_2]^3}. \tag{B.2}$$

Evaluating these at $\eta = 0$ and applying equation (11) provides the Laplace transformed moments

$$\frac{\langle\tilde{x}(s)\rangle}{v} = \frac{1}{s}\frac{\theta_2(s+\kappa)+k_1}{(s+\kappa+k')s+\kappa k_2} = \frac{1}{s}\frac{\theta_2(s+\kappa)+k_1}{(s+a+b)(s+a-b)}, \tag{B.3}$$

$$\frac{\langle\tilde{x}^2(s)\rangle}{2v^2} = \frac{1}{s}\frac{(s+\kappa+k_1)(\theta_2(s+\kappa)+k_1)}{[(s+\kappa+k')s+\kappa k_2]^2} = \frac{1}{s}\frac{(s+\kappa+k_1)(\theta_2(s+\kappa)+k_1)}{(s+a+b)^2(s+a-b)^2}. \tag{B.4}$$

The parameters $a = (\kappa+k')/2$ and $b^2 = a^2 - \kappa k_2$ were introduced to factorize the denominators. These equations can be inverted using the properties 15.164 (translation), 15.11.1 (integration), and 15.123 (differentiation) from Arfken (1985) after expansion in partial fractions. For the mean, the calculation is

$$\frac{2b}{v}\langle x\rangle = \big[\theta_2 + (k_1+\theta_2\kappa)\int_0^t dt\big]\mathcal{L}^{-1}\Big\{\frac{1}{s+a-b} - \frac{1}{s+a+b}; t\Big\} \tag{B.5}$$

$$= \Big[\theta_2 + \frac{k_1+\theta_2\kappa}{b-a}\Big]e^{(b-a)t} - \Big[\theta_2 - \frac{k_1+\theta_2\kappa}{a+b}\Big]e^{-(a+b)t} - \Big[\frac{k_1+\theta_2\kappa}{b-a} + \frac{k_1+\theta_2\kappa}{a+b}\Big]. \tag{B.6}$$

This equation rearranges to (13). The second moment (B.4) is

$$\frac{2b^2}{v^2}\langle x^2\rangle = \Big[\theta_2(\delta(t)+\partial_t) + (\theta_2(2\kappa+k_1)+k_1) + (\kappa+k_1)(\theta_2\kappa+k_1)\int_0^t dt\Big] \times \mathcal{L}^{-1}\Big\{\frac{1}{(s+a-b)^2} + \frac{1}{(s+a+b)^2} - \frac{1}{b(s+a-b)} + \frac{1}{b(s+a+b)}; t\Big\}. \tag{B.7}$$

This becomes

$$\frac{2b^3}{v^2}\langle x^2\rangle = \Big[\theta_2\partial_t + [\theta_2(2\kappa+k_1)+k_1] + (\kappa+k_1)(\theta_2\kappa+k_1)\int_0^t dt\Big] \times \Big((bt-1)e^{(b-a)t} + (bt+1)e^{-(a+b)t}\Big), \tag{B.8}$$

which evaluates to equation (14). $\sigma_x^2 = \langle x^2\rangle - \langle x\rangle^2$ derives the variance in equation (15).

C Limiting behavior of the moments

The easiest approach to extract the earlier results of Wu et al. (2019), Lisle et al. (1998), and H. A. Einstein (1937) for the moments and positional variance as limiting cases is to use the Laplace transformed moments (B.3) and (B.4) as a starting point.

An alternate approach is to take limits in the moments (13) and (14) directly, but this is more challenging. First we obtain the Wu et al. (2019) model as a limit case. These authors accounted for sediment burial considering motions to be instantaneous. They characterized sediment movement by a thin-tailed step length distribution, implicitly involving an infinite motion velocity. To obtain their conclusions on bedload diffusion, we send the mean duration of motion to zero ($1/k_2 \to 0$), the velocity to infinity ($v \to \infty$), and we hold the mean step distance $l = v/k_2$ constant. We use the initial condition that grains start at rest ($\theta_1 = 1$). Enacting these limits in equations (B.3) and (B.4) provides

$$\langle \tilde{x} \rangle = k_1 l \frac{1}{s(s+\kappa)}, \tag{C.1}$$

$$\langle \tilde{x}^2 \rangle = 2l^2 k_1 \frac{s+\kappa+k_1}{s(s+\kappa)^2}. \tag{C.2}$$

Inverting these equations and introducing the variables $c = lk_1$ (an effective velocity) and $D_d = l^2 k_1$ (a diffusivity) provides positional variance

$$\sigma_x^2(t) = \frac{2D_d(1-e^{-\kappa t})}{\kappa} + \frac{(1-e^{-2\kappa t}-2e^{-\kappa t}\kappa t)c^2}{\kappa^2}. \tag{C.3}$$

This is mathematically identical to the key result of Wu et al. (2019), providing two ranges of diffusion when $\kappa \ll k_1$. One is normal and the other, induced by sediment burial, is superdiffusive. From here, the H. A. Einstein (1937) result can be obtained by turning off the burial process ($\kappa \to 0$):

$$\sigma_x^2(t) = 2D_d t. \tag{C.4}$$

This represents a single range of normal diffusion (cf. Hubbell & Sayre, 1964; Nakagawa & Tsujimoto, 1976).

The Lisle et al. (1998) result can be obtained similarly. For this case, we neglect the burial process ($\kappa \to 0$) but retain the finite velocity and motion duration in equations (B.3) and (B.4). For the initial condition $\theta_1 = 1$, this provides

$$\langle \tilde{x} \rangle = vk_1 \frac{1}{s^2(s+k')}, \tag{C.5}$$

$$\langle \tilde{x}^2 \rangle = 2v^2 k_1 \frac{s+k_1}{s^3(s+k')^2}. \tag{C.6}$$

Inverting these equations provides the variance when $t \ll 1/\kappa$:

$$\sigma_x^2 = 2v^2 \frac{k_1}{k'^4}\Big(k_1\big[\frac{1}{2} - k't e^{-k't} - \frac{1}{2}e^{-2k't}\big] + k_2\big[-2 + k't + (2+k't)e^{-k't}\big]\Big). \tag{C.7}$$

This result encodes two stages of diffusion: at small times there is superdiffusion $\sigma_x^2 \propto t^\gamma$ with $\gamma = 2-3$ depending on the initial condition, and at longer times there is normal diffusion. This links back to the Einstein model in the limit of instantaneous steps: $1/k_2 \to 0$ and $v \to \infty$ while $v/k_2 = l$.

Finally, we examine the limit $t \to 0$ while leaving $\kappa \neq 0$. This will highlight the effect of initial conditions on the local range superdiffusion. By applying Tauberian theorems, we can argue the $t \to 0$ variance is determined by the $s \to \infty$ limits of (B.3) and (B.4) (e.g. Weeks & Swinney, 1998; Weiss, 1994). Expanding these equations in powers of $1/s \ll 1$ and inverting the resulting transforms gives

$$\langle x \rangle = v\theta_2 t + \frac{1}{2}v(\theta_1 k_1 - \theta_2 k_2)t^2 + O(t^3), \tag{C.8}$$

$$\langle x^2 \rangle = v^2\theta_2 t^2 + \frac{1}{3}v^2(\theta_1 k_1 - 2\theta_2 k_2)t^3 + O(t^4). \tag{C.9}$$

Taking only leading order terms for each option of θ_1 and θ_2, these equations provide the asymptotic ($t \to 0$) variance

$$\sigma_x^2(t) \sim v^2\theta_1\theta_2 t^2 + \frac{1}{3}v^2(\theta_1 k_1 + \theta_2 k_2)t^3. \tag{C.10}$$

This equation shows the effect of initial conditions on the diffusion characteristics of the local range.

Acknowledgments

J. Pierce acknowledges helpful exchanges with Eduardo Daly and Peter Hänggi during the early stages of this work. He would like to thank Melinda Saunders and Leonardo Golubovic for their careful guidance in mathematics through the years. M. Hassan is supported by an NSERC Discovery grant. The Python simulation code is available at `https://github.com/kevinkayaks/rw-diffu`.

References

Ancey, C., Böhm, T., Jodeau, M., & Frey, P. (2006). Statistical description of sediment transport experiments. *Physical Review E - Statistical, Nonlinear, and Soft Matter Physics*, *74*(1), 1–14. doi: 10.1103/PhysRevE.74.011302

Arfken, G. (1985). *Mathematical Methods for Physicists*. Academic Press, Inc. doi: 10.1063/1.3062258

Barik, D., Ghosh, P. K., & Ray, D. S. (2006). Langevin dynamics with dichotomous noise; Direct simulation and applications. *Journal of Statistical Mechanics: Theory and Experiment*(3). doi: 10.1088/1742-5468/2006/03/P03010

Berezhkovskii, A. M., & Weiss, G. H. (2002). Detailed description of a two-state non-Markov system. *Physica A: Statistical Mechanics and its Applications*, *303*(1-2), 1–12. doi: 10.1016/S0378-4371(01)00431-9

Berkowitz, B., Cortis, A., Dentz, M., & Scher, H. (2006). Modeling Non-fickian transport in geological formations as a continuous time random walk. *Reviews of Geophysics*, *44*(2), 1–49. doi: 10.1029/2005RG000178

Bialik, R. J., Nikora, V. I., & Rowiński, P. M. (2012). 3D Lagrangian modelling of saltating particles diffusion in turbulent water flow. *Acta Geophysica*, *60*(6), 1639–1660. doi: 10.2478/s11600-012-0003-2

Bradley, N. D. (2017). Direct Observation of Heavy-Tailed Storage Times of Bed Load Tracer Particles Causing Anomalous Superdiffusion. *Geophysical Research Letters*, *44*(24), 12,227–12,235. doi: 10.1002/2017GL075045

Church, M. (2006). Bed Material Transport and the Morphology of Alluvial River Channels. *Annual Review of Earth and Planetary Sciences*, *34*(1), 325–354. Retrieved from `http://www.annualreviews.org/doi/10.1146/annurev.earth.33.092203.122721` doi: 10.1146/annurev.earth.33.092203.122721

Codling, E. A., Plank, M. J., & Benhamou, S. (2008). Random walk models in biology. *Journal of the Royal Society Interface*, *5*(25), 813–834. doi: 10.1098/rsif.2008.0014

Daly, E., & Porporato, A. (2010). Effect of different jump distributions on the dynamics of jump processes. *Physical Review E - Statistical, Nonlinear, and Soft Matter Physics*, *81*(6), 1–10. doi: 10.1103/PhysRevE.81.061133

Dhont, B., & Ancey, C. (2018). Are Bedload Transport Pulses in Gravel Bed Rivers Created by Bar Migration or Sediment Waves? *Geophysical Research Letters*, *45*(11), 5501–5508. doi: 10.1029/2018GL077792

Einstein, A. (1905). Brownian Movement. *Biotropica*, *1*. doi: 10.5167/uzh-53657

Einstein, H. A. (1937). *Bed-load transport as a probability problem* (Unpublished doctoral dissertation). ETH Zurich.

Ettema, R., & Mutel, C. F. (2004). Hans Albert Einstein: Innovation and Compromise in Formulating Sediment Transport by Rivers. *Journal of Hydraulic Engi-*

neering, *130*(6), 477–487. doi: 10.1061/(ASCE)0733-9429(2004)130:6(477)

Fan, N., Singh, A., Guala, M., Foufoula-Georgiou, E., & Wu, B. (2016). Exploring a semimechanistic episodic Langevin model for bed load transport: Emergence of normal and anomalous advection and diffusion regimes. *Water Resources Research*, *52*(4), 3787–3814. doi: 10.1002/2016WR018704.Received

Ferguson, R. I., Bloomer, D. J., Hoey, T. B., & Werritty, A. (2002). Mobility of river tracer pebbles over different timescales. *Water Resources Research*, *38*(5), 3–1–3–8. doi: 10.1029/2001wr000254

Ferguson, R. I., & Hoey, T. B. (2002). Long-term slowdown of river tracer pebbles: Generic models and implications for interpreting short-term tracer studies. *Water Resources Research*, *38*(8), 17–1–17–11. doi: 10.1029/2001wr000637

Gaeuman, D., Stewart, R., Schmandt, B., & Pryor, C. (2017). Geomorphic response to gravel augmentation and high-flow dam release in the Trinity River, California. *Earth Surface Processes and Landforms*, *42*(15), 2523–2540. doi: 10.1002/esp.4191

Ganti, V., Meerschaert, M. M., Foufoula-Georgiou, E., Viparelli, E., & Parker, G. (2010). Normal and anomalous diffusion of gravel tracer particles in rivers. *Journal of Geophysical Research: Earth Surface*, *115*(F2), n/a–n/a. Retrieved from `http://doi.wiley.com/10.1029/2008JF001222` doi: 10.1029/2008JF001222

Giddings, J. C., & Eyring, H. (1955). A molecular dynamic theory of chromatography. *Journal of Physical Chemistry*, *59*(5), 416–420.

Gordon, R., Carmichael, J. B., & Isackson, F. J. (1972). Saltation of Plastic Balls in a 'One-Dimensional' Flume. *Water Resources Research*, *8*(2), 444–458. doi: 10.1029/WR008i002p00444

Haschenburger, J. K. (2013). Tracing river gravels: Insights into dispersion from a long-term field experiment. *Geomorphology*, *200*, 121–131. Retrieved from `http://dx.doi.org/10.1016/j.geomorph.2013.03.033` doi: 10.1016/j.geomorph.2013.03.033

Hassan, M. A., & Bradley, D. N. (2017). Geomorphic controls on tracer particle dispersion in gravel bed rivers. In *Gravel-bed rivers: Processes and disasters* (pp. 159–184). New York, NY: John Wiley & Sons Ltd. doi: 10.16719/j.cnki.1671-6981.2015.03.007

Hassan, M. A., & Church, M. (1994). Vertical mixing of coarse particles in gravel bed rivers: A kinematic model. *Water Resources Research*, *30*(4), 1173–1185. doi: 10.1029/93WR03351

Hassan, M. A., Church, M., & Schick, A. P. (1991). Distance of movement of coarse particles in gravel bed streams. *Water Resources Research*, *27*(4), 503–511. doi: 10.1029/90WR02762

Hassan, M. A., Voepel, H., Schumer, R., Parker, G., & Fraccarollo, L. (2013). Displacement characteristics of coarse fluvial bed sediment. *Journal of Geophysical Research: Earth Surface*, *118*(1), 155–165. doi: 10.1029/2012JF002374

Hubbell, D. W., & Sayre, W. W. (1964). Sand Transport Studies with Radioactive Tracers. *J. Hydr. Div.*, *90*(HY3), 39–68.

Jeon, J. H., Monne, H. M. S., Javanainen, M., & Metzler, R. (2012). Anomalous diffusion of phospholipids and cholesterols in a lipid bilayer and its origins. *Physical Review Letters*, *109*(18), 1–5. doi: 10.1103/PhysRevLett.109.188103

Kasprak, A., Wheaton, J. M., Ashmore, P. E., Hensleigh, J. W., & Peirce, S. (2014). The relationship between particle travel distance and channel morphology : Results from physical models of braided rivers. *Journal of Geophysical Research : Earth Surface*, *120*, 55–74. doi: 10.1002/2014JF003310.Received

Kittel, C. (1958). *Elementary Statistical Physics*. R.E. Krieger Pub. Co.

Lajeunesse, E., Malverti, L., & Charru, F. (2010). Bed load transport in turbulent flow at the grain scale: Experiments and modeling. *Journal of Geophysical Research: Earth Surface*, *115*(4). doi: 10.1029/2009JF001628

Lisle, I. G., Rose, C. W., Hogarth, W. L., Hairsine, P. B., Sander, G. C., & Parlange, J.-Y. (1998). Stochastic sediment transport in soil erosion. *Journal of Hydrology*, *204*, 217–230.

Macklin, M. G., Brewer, P. A., Hudson-Edwards, K. A., Bird, G., Coulthard, T. J., Dennis, I. A., ... Turner, J. N. (2006). A geomorphological approach to the management of rivers contaminated by metal mining. *Geomorphology*, *79*(3-4), 423–447. doi: 10.1016/j.geomorph.2006.06.024

Malmon, D. V., Dunne, T., & Reneau, S. L. (2003). Stochastic Theory of Particle Trajectories through Alluvial Valley Floors. *The Journal of Geology*, *111*(5), 525–542. doi: 10.1086/376764

Malmon, D. V., Reneau, S. L., Dunne, T., Katzman, D., & Drakos, P. G. (2005). Influence of sediment storage on downstream delivery of contaminated sediment. *Water Resources Research*, *41*(5), 1–17. doi: 10.1029/2004WR003288

Marcum, J. (1960). A statistical theory of target detection by pulse radar. *IRE Trans. Inform. Theory*, *6*, 59–268.

Martin, R. L., Jerolmack, D. J., & Schumer, R. (2012). The physical basis for anomalous diffusion in bed load transport. *Journal of Geophysical Research: Earth Surface*, *117*(1), 1–18. doi: 10.1029/2011JF002075

Martin, R. L., Purohit, P. K., & Jerolmack, D. J. (2014). Sedimentary bed evolution as a mean-reverting random walk: Implications for tracer statistics. *Geophysical Research Letters*, *41*(17), 6152–6159. doi: 10.1002/2014GL060525

Metzler, R., & Klafter, J. (2000). The random walk's guide to anomalous diffusion: A fractional dynamics approach. *Physics Report*, *339*(1), 1–77. doi: 10.1016/S0370-1573(00)00070-3

Molina-Garcia, D., Sandev, T., Safdari, H., Pagnini, G., Chechkin, A., & Metzler, R. (2018). Crossover from anomalous to normal diffusion: Truncated power-law noise correlations and applications to dynamics in lipid bilayers. *New Journal of Physics*, *20*(10). doi: 10.1088/1367-2630/aae4b2

Montroll, E. W., & Weiss, G. H. (1965). Random Walks on Lattice. II. *Jounral of Mathematical Physics*, *6*, 167–181.

Nakagawa, H., & Tsujimoto, T. (1976). On Probabilistic Characteristics of Motion of Individual Sediment Particles on Stream Beds. In *Hydraulic problems solved by stochastic methods: Second international iahr symposium on stochastic hydraulics* (pp. 293–320). Lund, Sweden.

Nakagawa, H., & Tsujimoto, T. (1980). Sand bed instability due to bed load motion. *Journal of the Hydraulics Division-ASCE*.

Nikora, V., Habersack, H., Huber, T., & McEwan, I. (2002). On bed particle diffusion in gravel bed flows under weak bed load transport. *Water Resources Research*, *38*(6), 1–9. Retrieved from `http://doi.wiley.com/10.1029/2001WR000513` doi: 10.1029/2001WR000513

Nikora, V., Heald, J., Goring, D., & McEwan, I. (2001). Diffusion of saltating particles in unidirectional water flow over a rough granular bed. *Journal of Physics A: Mathematical and General*, *34*(50). doi: 10.1088/0305-4470/34/50/103

Olinde, L., & Johnson, J. P. L. (2015). Using RFID and accelerometer-embedded tracers to measure probabilities of bed load transport, step lengths, and rest times in a mountain stream. *Water Resources Research*, *51*, 7572–7589. doi: 10.1002/2014WR016259

Phillips, C. B., Martin, R. L., & Jerolmack, D. J. (2013). Impulse framework for unsteady flows reveals superdiffusive bed load transport. *Geophysical Research Letters*, *40*(7), 1328–1333. doi: 10.1002/grl.50323

Prudnikov, A., Brychkov, Y. A., & Marichev, O. (1992). *Integrals and Series: Volume 5: Inverse Laplace Transforms*. Gordon and Breach Science Publishers.

Pyrce, R. S., & Ashmore, P. E. (2005). Bedload path length and point bar development in gravel-bed river models. *Sedimentology*, *52*(4), 839–857. doi: 10.1111/j.1365-3091.2005.00714.x

Reynolds, A., & Rhodes, C. (2009). The Levy flight paradigm: random search patterns and mechanisms. *Ecology*, *90*(4), 877–887.

Schmidt, M. G., Sagués, F., & Sokolov, I. M. (2007). Mesoscopic description of reactions for anomalous diffusion: A case study. *Journal of Physics Condensed Matter*, *19*(6). doi: 10.1088/0953-8984/19/6/065118

Sokolov, I. M. (2012). Models of anomalous diffusion in crowded environments. *Soft Matter*, *8*(35), 9043–9052. doi: 10.1039/c2sm25701g

Taylor, G. I. (1920). Diffusion by continuous movements. *Proceedings of the London Mathematical Society*, *s2-20*(1), 196–212.

Temme, N. M. (1996). *Special functions: an introduction to the classical functions of mathematical physics*. John Wiley & Sons Ltd.

Vallaeys, V., Tyson, R. C., Lane, W. D., Deleersnijder, E., & Hanert, E. (2017). A Lévy-flight diffusion model to predict transgenic pollen dispersal. *Journal of the Royal Society Interface*, *14*(126). doi: 10.1098/rsif.2016.0889

Voepel, H., Schumer, R., & Hassan, M. A. (2013). Sediment residence time distributions: Theory and application from bed elevation measurements. *Journal of Geophysical Research: Earth Surface*, *118*(4), 2557–2567. doi: 10.1002/jgrf.20151

Weeks, E. R., & Swinney, H. L. (1998). Anomalous diffusion resulting from strongly asymmetric random walks. *Physical Review E - Statistical Physics, Plasmas, Fluids, and Related Interdisciplinary Topics*, *57*(5), 4915–4920. doi: 10.1103/PhysRevE.57.4915

Weiss, G. H. (1976). The two-state random walk. *Journal of Statistical Physics*, *15*(2), 157–165. doi: 10.1007/BF01012035

Weiss, G. H. (1994). *Aspects and applications of the random walk*. Amsterdam: North Holland.

Wu, Z., Foufoula-Georgiou, E., Parker, G., Singh, A., Fu, X., & Wang, G. (2019). Analytical Solution for Anomalous Diffusion of Bedload Tracers Gradually Undergoing Burial. *Journal of Geophysical Research: Earth Surface*, *124*(1), 21–37. doi: 10.1029/2018JF004654

Yang, C. T., & Sayre, W. W. (1971). Stochastic model for sand dispersion. *Journal of the Hydraulics Division, ASCE*, *97*(HY2).

Yang, X. R., & Wang, Y. (2019). Ubiquity of anomalous transport in porous media: Numerical evidence, continuous time random walk modelling, and hydrodynamic interpretation. *Scientific Reports*, *9*(1), 1–11. Retrieved from `http://dx.doi.org/10.1038/s41598-019-39363-3` doi: 10.1038/s41598-019-39363-3

Yano, K. (1969). Tracer Studies on the Movement of Sand and Gravel. In *Proceedings of the 12th congress iahr, vol 2.* (pp. 121–129). Kyoto, Japan.

Yano, K., Tsuchiya, Y., & Michiue, M. (1969). Studies on the Sand Transport in Streams with Tracers. *Bull. Disas. Prev. Res. Inst. Kyoto Univ.*, *18*(Part 3, No. 141).

Zhang, Y., Meerschaert, M. M., & Packman, A. I. (2012). Linking fluvial bed sediment transport across scales. *Geophysical Research Letters*, *39*(20), 1–6. doi: 10.1029/2012GL053476